Available online at www.sciencedirect.com
ScienceDirect
Catalysis Today 120 (2007) 168–173
CATALYSIS TODAY
www.elsevier.com/locate/cattod

Nanoclusters of silver doped in zeolites as photocatalysts

Howard H. Patterson *, Robert S. Gomez, Haiyan Lu, Renante L. Yson

Department of Chemistry, University of Maine, Orono, ME 04469, United States

Available online 14 September 2006

Abstract

Nanoclusters of silver and iron ions doped in Y zeolite and sodalite have been prepared. Photoluminescence spectra of Ag-Y zeolite, Ag/Fe_2O_3-Y zeolite, Ag-sodalite, and Ag/Fe_2O_3-sodalite were obtained from 4.5 to 298 K and revealed the formation of different kinds of silver clusters in the zeolite hosts. The amount of silver and iron in the corresponding material were determined using atomic absorption spectroscopy. The purity and unit cell structure of each catalysts was determined using X-ray powder diffraction analysis. It was found that while the structure of the support materials remained relatively intact after the incorporation of Ag^+ and Fe^{3+} onto the supports, differences in the structure of the support corresponded with differences in cluster size and composition. It was also found that adding Fe_2O_3 to Ag-Y zeolite shifted the observed Ag cluster photoluminescence to longer wavelengths, while Ag-sodalite remains largely unaffected by the addition of Fe_2O_3. This further supports the conclusion that the structure of the support material plays a major role in cluster formation.

Keywords: Nanoclusters; Photocatalysis; X-ray diffraction; Silver; Zeolites

1. Introduction

The tendency of silver ions to bond together and form nanosized clusters has long been known [1–10]. The properties of these silver nanoclusters are affected by its environment, and in particular, the type of zeolite lattice used to support the silver clusters [10–13]. There is great interest in silver because of its importance in photocatalytic processes and because of its unique catalytic properties [10,14]. Studying how silver aggregates and forms clusters is important since these clusters may play a role in heterogeneous photocatalysis [10,15–20]. For example, a study of a photocatalytic process to coat silver clusters on titanium dioxide with emphasis on control of the morphology of coated silver clusters has been done [14].

There are several methods that exist on how silver can be incorporated into the cages and channels and onto the surfaces of zeolites. These methods include hydrothermal methods, ion exchange, vacuum dehydration and X-ray irradiation. Different silver clusters have been impregnated into Y-zeolite. Some examples include dimers (Ag_2, Ag_2^+), trimers (Ag_3^{2+}), and hexamers (Ag_6^{4+}) [2,6,7,10,21,22]. Kim and Seff have used single crystal X-ray diffraction techniques to determine the structure of the uncharged octahedral hexasilver clusters, Ag_6^0, in sodalite cavities [10]. They assigned a neutral charge to the cluster because the Ag–Ag distance is similar to that found in Ag metal. The photoluminescence properties of Ag clusters on zeolites have been extensively studied, and many have reported on their use as photocatalysts for the decomposition of organic matter and pesticides [23–25]. In our laboratory, we have prepared Ag nanoclusters and dicyanoargentate nanoclusters doped in A zeolite, Y zeolite, and ZSM-5 using ion exchange techniques and have successfully used the synthesized compounds as photocatalysts in the decomposition of NO_x, malathion, and carbaryl [26–29].

The addition of a second metal to homometallic catalysts and photocatalysts is also of interest to scientists because it could potentially lead to the enhancement of several properties such as an increase in the catalysts' reactivity and its resistance to poisoning [30,31]. Previous research had been done using zeolites doped with two different metals or metal oxides as catalysts and photocatalysts, and in many instances the reactivity, selectivity, and/or the stability of the catalysts have all been improved [32–34].

In this study, we report the synthesis and luminescence properties of several Ag and Ag/Fe_2O_3 doped zeolites and discuss their possible use as photocatalysts. Based on photoluminescence data, atomic absorbance data and X-ray

* Corresponding author. Tel.: +1 207 581 1169; fax: +1 207 581 1191.

0920-5861/$ – see front matter
doi:10.1016/j.cattod.2006.07.057

powder diffraction data, we will show that Ag doped zeolites form dimer and trimer Ag nanoclusters, and that cluster composition, structure and distribution is affected by the type of zeolite support and the presence of a second metal oxide. The catalytic studies using these materials are currently being undertaken and we already have promising preliminary results. The results will appear in a separate publication.

2. Experimental

Aluminum hydroxide, NaBr, NaOH were purchased from Sigma Aldrich, CBV 300 Y-Zeolite from Zeolyst International, LUDOX AS-40 colloidal silica solution from Grace Davison, Fe_2O_3 from Fisher, and $AgNO_3$ from Spectrum Chemical. All reagents were used as received. Deionized distilled water was used in all preparations. NaBr sodalite was synthesized using hydrothermal methods as described in literature [35,36] and was analyzed for purity using XRD with instruments and methods described in Section 2.4. All iron-containing zeolites are referred to as Fe_2O_3 since this is the most common oxidation state of iron and has been shown to be present in iron doped Y zeolite [37,38].

2.1. Synthesis of Ag-sodalite

The synthesis of Ag-sodalite was carried out using common ion exchange methods. A minimal amount of concentrated NH_3 solution was added slowly to an aqueous solution of $AgNO_3$ until the mixture turned from clear to dark brown and back to clear, indicating the formation of $Ag(NH_3)_2^+$. The solution was heated to 70 °C and NaBr sodalite was added in the dark. The mixture was stirred in the dark for 48 h, after which it was filtered and washed three times with deionized water. The product was dried at 110 °C for 24 h, then calcined at 500 °C for 2 h. Yield: 4.59 g.

2.2. Synthesis of Ag/Fe_2O_3-sodalite

Ag/Fe_2O_3-sodalite was prepared in a similar fashion as Ag-sodalite, with the only difference being the addition of Fe_2O_3 powder to the solution before adding NaBr sodalite to the mixture. Yield: 2.01 g.

2.3. Syntheses of Ag-Y zeolite and Ag/Fe_2O_3-Y zeolite

These catalysts were synthesized in a similar manner to Ag-sodalite and Ag/Fe_2O_3-sodalite using Zeolyst CBV 300 Y zeolite as the support material instead of sodalite. Yield: 4.20 g (Ag-Y zeolite); 4.86 g (Ag/Fe_2O_3-Y zeolite).

2.4. Characterization

Steady state luminescence experiments were performed using a Photon Technology International Model Quantamaster-1 spectrofluorimeter equipped with a 75 W lamp and dual excitation monochromators. All emission and excitation spectra are uncorrected unless otherwise stated. Low temperature measurements were done using a Model LT-3-110 Heli-Tran cryogenic liquid transfer system equipped with a temperature controller. Powder samples of the zeolites were attached to a copper surface that was then attached to the transfer tube for low temperature measurements. The amount of silver and iron in the zeolites were determined by atomic absorption spectroscopy using a Smith-Hieftje Model 857 Atomic Absorption spectrometer with flame ionizer. Each zeolite catalyst was digested with a 1:1:1 mixture of HF/HCl/HNO_3 and diluted with deionized water before analysis. Standard solutions were prepared using analytical grade $AgNO_3$ and Fe_2O_3. X-ray powder diffraction data was collected at 298 K using a fully automated Scintag, Inc. X-2 Advanced Diffraction XRD system using Cu K_α radiation (1.540562 Å). The samples were crushed into a fine powder before being distributed on a salt plate with as little topology as possible and scanned from 8° to 70° in 2θ. The crystallinity of the doped materials remained largely unchanged from that of the undoped zeolites.

3. Results and discussion

There are many reports on the catalytic activity of silver clusters [11–13,15,17,18,20,22,26–29,39–45]. Several types of support have been used including SiO_2, TiO_2 and zeolites [10,19,26,46,47]. In our laboratory, we have successfully prepared and characterized Ag nanoclusters and dicyanoargentate nanoclusters doped in A zeolite, Y zeolite, and ZSM-5 and have successfully used the synthesized compounds as catalysts in the photodecomposition of NO_x, malathion, and carbaryl [26–29]. We have also proposed a reaction mechanism for the photocatalytic process. While silver in its ground electronic state is a d^{10} closed-shell ion and is relatively unreactive, silver ions can be easily photoexcited to an open shell d^9s^1 or d^9p^1 configuration, thus changing its reactivity. This is because open shell species are more reactive than closed shell ions. Theoretical calculations on two $Ag(CN)_2^-$ ions showed that the potential curve of the ground state has a shallow minimum, whereas the lowest excited state has a deep minimum indicative of the formation of Ag–Ag bonds [48,49]. Since excimer and exciplex forms of silver complexes have been suggested as possible intermediates in photocatalytic cycles, the increased stability of the excited state that result from the formation of strong Ag–Ag interactions provides a driving force for the photodecomposition reactions for which these catalysts are used. The formation of $Ag(CN)_2^-$ clusters in zeolite A have also been verified by resonance Raman spectroscopy [26,28].

The amount of silver and iron in each of the zeolites investigated in this study were analyzed by atomic absorption spectroscopy. The results are summarized in Table 1. Ag-sodalite has the highest amount of silver (35.5 wt.%), while Ag/Fe_2O_3-sodalite and Ag-Y zeolite contain roughly half of this amount. Also, Ag/Fe_2O_3-sodalite (23.5 wt.%) has roughly twice the amount of iron as Ag/Fe_2O_3-Y zeolite (11.9 wt.%). Because the concentration of the dopants inside the zeolite host affects the type of clusters that eventually form, it is expected

Table 1
Silver and iron content (wt.%) of the different zeolite samples

Zeolite	% Ag	% Fe
Ag-sodalite	35.5	–
Ag-Y zeolite	16.6	–
Ag/Fe_2O_3-sodalite	18.4	23.5
Ag/Fe_2O_3-Y zeolite	9.1	11.9

that different sized clusters (dimers, trimers, etc.) will be found in the four homometallic and bimetallic zeolites reported here. Larger clusters are expected to form where the silver loading is high, whereas smaller clusters should predominate samples containing a smaller concentration of dopant material. In this case, dimers should be the predominant form of silver clusters in Ag-Y zeolite, being the one with the lowest silver loading, and trimers and larger oligomers should predominate Ag-sodalite, being the one with the highest silver loading.

Fig. 1 shows the emission spectra of $Ag(CN)_2^-$ doped in KCl single crystals at different excitation wavelengths at 77 K. Three major luminescence bands are seen at 290, 340, and 412 nm (labeled as A–C). It can be seen that emission maxima are strongly dependent on the excitation wavelengths and each of the bands become dominant over the others by selecting a characteristic excitation wavelength. The different emission bands are therefore resolved by site-selective excitation. Because of the known sensitivity of d^{10} luminescence to metal–metal interactions, the bands seen in Fig. 1 are most probably due to aggregates of dicyanoargentates in the KCl lattice [8,9,48–52]. The different emission bands are assigned to their corresponding excimers and exciplexes (monomers, dimers and trimers of $Ag(CN)_2^-$) that form in the KCl host lattice. The high energy emission (band A) near 290 nm is attributed to a $^*[Ag(CN)_2^-]_2$ excimer. Bands B and C centered at 340 and 412 nm, respectively, are attributed to the formation of angular and linear geometrical isomers of $^*[Ag(CN)_2^-]_3$ trimers. The $Ag(CN)_2^-$ are distributed in a linear ($D_{\infty h}$) arrangement in band C and angular (C_{2v}) in band B. The luminescence energy depends on the identity of the $[Ag(CN)_2^-]_n$ emissive exciplex, and there is an observed decrease in luminescence energy as the number of $Ag(CN)_2^-$ aggregates increase. This is similar to results we have reported previously [48], and both the experimental and the theoretical results suggest the formation of Ag–Ag-bonded excimers and exciplexes between adjacent $Ag(CN)_2^-$ ions in the host lattice. This observation is not limited to the solid state but can also be seen in solution. We have reported on the formation of metal–metal bonded oligomers in aqueous and methanolic solutions of dicyanoargentate ions of different concentrations where dimers, trimers, and oligomers of dicyanoargentate are seen at room temperature and 77 K [9].

Fig. 2 shows the excitation spectra for each emission band of $Ag(CN)_2^-$/KCl single crystals with the emission monitored at wavelengths that correspond to each of the emission bands. It can be seen that a different excitation peak is associated with each emission band. The peaks within different excitation bands are most likely due to different orientations of $Ag(CN)_2^-$ units in the crystal lattice. These results lead to the conclusion that the type of Ag^+ clusters formed are largely determined by the surroundings and the host lattice structure.

Because of the potential that exists for the use of silver clusters in photocatalysis, we decided to extend our study on excimers and exciplexes by incorporating silver ions in zeolite supports and including a second metal oxide on the supports. Similar to the $Ag(CN)_2^-$ doped in KCl, room and low temperature steady state luminescence experiments were performed on Ag-sodalite, Ag/Fe_2O_3-sodalite, Ag-Y zeolite, and Ag/Fe_2O_3-Y zeolite.

Fig. 3 shows the luminescence spectra of silver doped Y-zeolite at 77 K. It can be seen from the figure that the luminescence is very similar to that observed in $Ag(CN)_2^-$/KCl

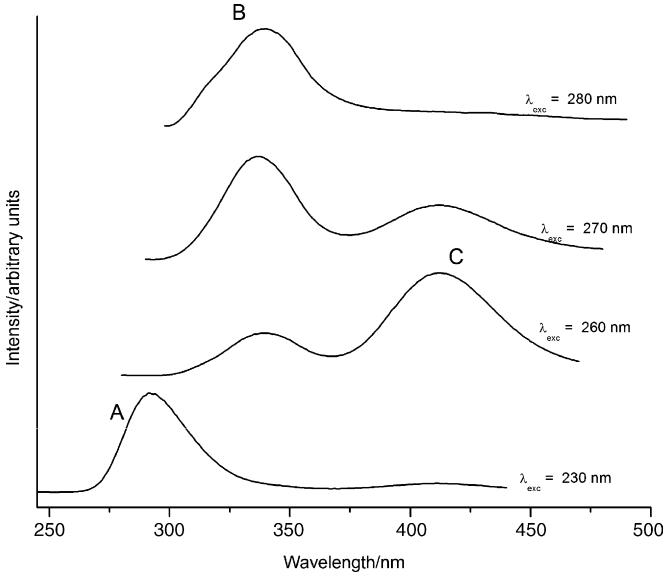

Fig. 1. Emission spectra of a $KAg(CN)_2$/KCl crystal at 77 K with different excitation wavelengths. Intensities are not comparable between different spectra.

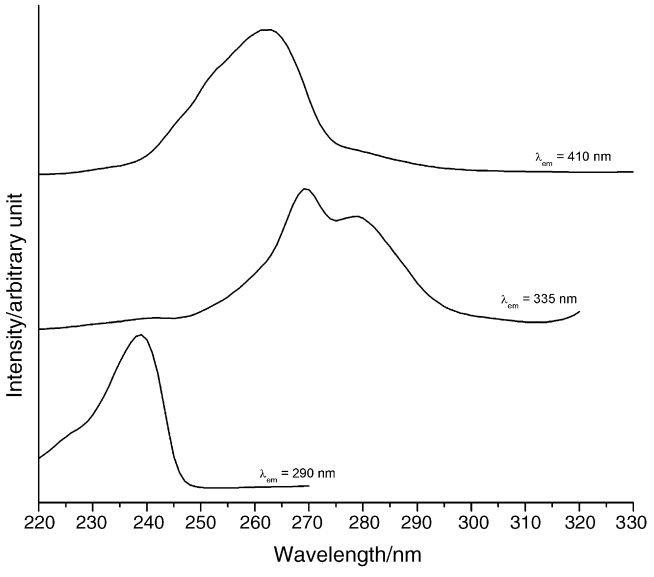

Fig. 2. Excitation spectra of a $KAg(CN)_2$/KCl crystal at 77 K. Intensities are not comparable between different spectra.

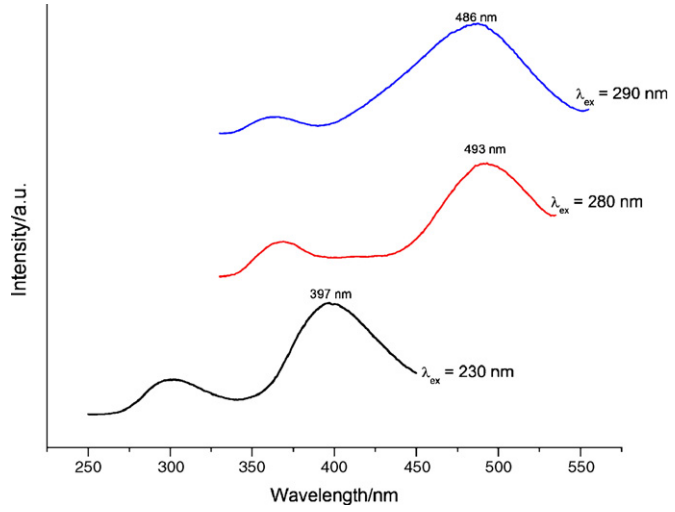

Fig. 3. Emission spectra of Ag-doped zeolite-Y at 77 K with different excitation wavelengths. The intensities are not comparable between the different spectra.

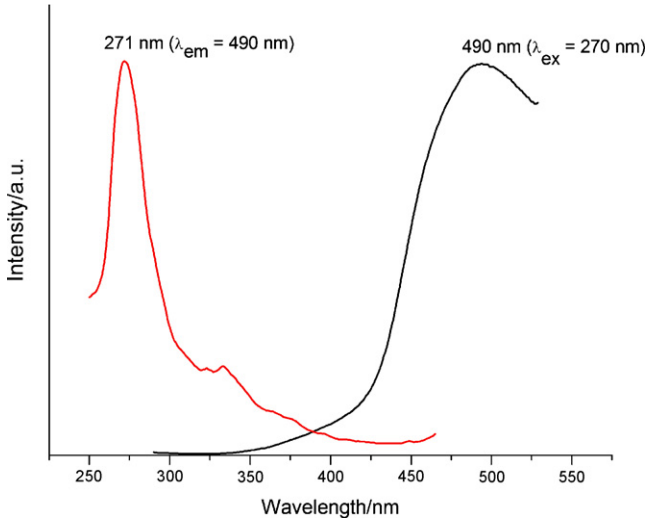

Fig. 4. Emission and excitation spectra of Ag-doped sodalite at 77 K.

crystals, and that the luminescence spectra is strongly dependent upon the excitation wavelength. Thus we can assign the different emission bands to the silver clusters in a manner like those in $Ag(CN)_2^-$ doped in KCl crystals. A low energy and a high energy band is seen for each excitation wavelength. The emissions at ca. 300 and 397 nm (λ_{ex} = 230 nm), 368 and 493 nm (λ_{ex} = 280 nm), and 360 and 486 nm (λ_{ex} = 290 nm) are assigned to $*[Ag^+]_n$ dimer and trimer aggregates within the zeolite. The tentative assignment the different silver clusters are shown in Table 2. For each case, the low energy band has higher intensity than the high energy band.

The emission and excitation spectra of Ag-sodalite are shown in Fig. 4. In contrast to Ag-Y zeolite, the emission spectrum shows only one maximum at 490 nm when excited at 270 nm. This lower energy emission does not change significantly with temperature (Fig. 6) and it is assigned to the formation of $*[Ag^+]_3$ trimers in the zeolite. These results agree well with the silver loading in each zeolite sample as determined by atomic absorption spectroscopy. Thus, in Ag-Y zeolite, where the silver loading is around 17%, both dimers and trimers of silver are seen. The concentration of the dopant is still high so that there are still areas containing large amounts of silver and permit the formation of trimers. In Ag-sodalite, the concentration of dopant is high enough such that only trimers and higher oligomers are seen. It is also interesting to note that there is no significant change in the emission spectra as the temperature is increased from 77 K to room temperature. From these results, it can be seen that the type of silver clusters can be easily controlled in each zeolite via control of stoichiometry, and can be easily probed using photoluminescence spectroscopy. Furthermore, because different types of silver clusters form on sodalite and Y-zeolite, it is expected that this will impact their photocatalytic properties.

The effect of adding a second dopant on the luminescence behavior of the Ag-Y zeolite and Ag-sodalite was also studied. Ag-Y zeolite was doped with Fe_2O_3 and its photoluminescence spectra was determined (Fig. 5). Comparing the emission spectra of Ag-Y zeolite and Ag/Fe_2O_3-Y zeolite, we observed that the emissions seen when the sample is excited at 230 nm remain largely unchanged. However, the emissions seen when the sample is excited at 280 and 290 nm exhibited a major change. When the sample is cooled to 77 K, broad, structureless emission maximum centered at 410 and 428 nm are seen when the sample is excited at 280 and 290 nm, respectively (Fig. 5).

Table 2
Assignment of the luminescence band for silver clusters doped in KCl single crystal, Y-zeolite, and sodalite

Luminescence band	λ_{em} (nm)	λ_{ex} (nm)	Assignment[a]
A	270–290	225–240	$*[Ag^+]_2$
B	310–370	270–290	$*[Ag^+]_3$—angular
C	390–420	250–270	$*[Ag^+]_3$—linear
–	450–540	260–300	Delocalized exciplexes

[a] The peaks seen at each luminescent band are due to cluster ions present in different environments in the zeolite lattice.

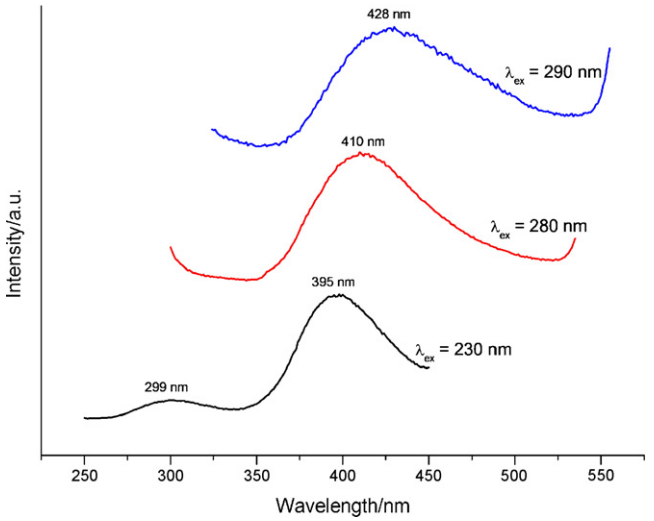

Fig. 5. Emission spectra of Ag–Fe doped Y-zeolite at 77 K at different excitation wavelengths.

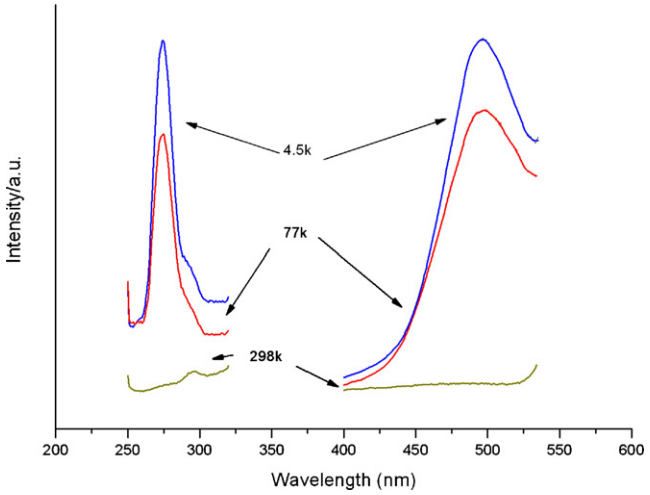

Fig. 6. Emission and excitation spectra of Ag-doped sodalite at 4.5, 77, and 298 K.

We did not observe any significant luminescence due to iron oxide from the iron oxide-doped Y-zeolite when it was excited at the same wavelengths. The luminescence intensity due to silver is high and masks any luminescence contribution from iron oxide. Thus, the addition of Fe_2O_3 to the Ag-Y zeolite catalyst resulted in a shift to shorter wavelengths of the observed emission maxima when the sample was excited at 280 and 290 nm. These findings suggest that the addition of Fe_2O_3 to the Ag-Y zeolite catalyst either alters the Ag cluster in a manner that makes the cluster photocatalytically active using higher energy radiation or forms new clusters with Fe_2O_3 incorporated into the Ag cluster.

This phenomenon does not take place on the sodalite-supported zeolite and exciting the sodalite-supported zeolite with 280 and 290 nm light did not significantly alter the position of the observed emission maxima of the sample. Fig. 6 shows the emission spectra of Ag-doped sodalite at different temperatures. The emission maximum centered at 495 nm varies as a function of temperature and its intensity increases as the temperature decrease. Fig. 7 shows the emission and excitation spectra of Ag/Fe-doped sodalite at different temperatures. Again, the emission intensity varies as a function of temperature. However, the emission maxima for both Ag-doped and Ag/Fe-doped zeolite remained essentially the same at 495 nm. No significant luminescence due to iron oxide was observed from the iron oxide-doped sodalite at these excitation wavelengths. The luminescence intensity due to silver is high and masks any luminescence contribution from iron oxide. This result indicates that addition of Fe_2O_3 to the Ag-doped sodalite material has no effect on the size of silver clusters that form, in contrast to that observed for Ag/Fe-doped Y-zeolite.

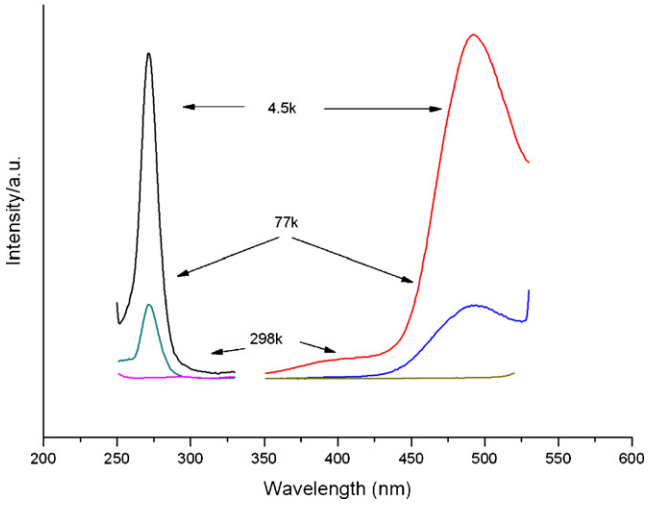

Fig. 7. Emission and excitation spectra of Ag–Fe doped sodalite at 4.5, 77, and 298 K.

4. Conclusions

This study reports on the synthesis and luminescence properties of several Ag and Ag/Fe_2O_3 doped zeolites. Photoluminescence spectra obtained at different temperatures revealed the presence of Ag nanoclusters in the zeolite channels consisting of various cluster sizes. From these spectra, we found that the distribution of the Ag clusters depends largely on the type of zeolite used in the synthesis. Our results also showed that the presence of a second dopant such as Fe_2O_3 in Ag-doped zeolites can affect the luminescence spectrum of the material and consequently, the cluster distribution, depending on the structure of the zeolite support. Specifically, the presence of Fe_2O_3 changes the electronic structure of Ag clusters doped in Y zeolite, while the presence of Fe_2O_3 does not change the electronic structure of Ag clusters doped in sodalite. This is important because it is believed that the cluster distribution and the size and composition of clusters that form affects the photocatalytic properties of the synthesized catalyst. With a greater understanding of a how a second dopant, particularly a metal oxide, affects the electronic and physical structure of photocatalytic centers in zeolite supports, more reactive, selective, and stable catalysts can be designed and synthesized for a range of important reactions. Catalytic studies using these materials are currently being undertaken and the results will appear in a separate publication.

Acknowledgements

The authors would like to acknowledge the US Department of the Army and the National Science Foundation for providing financial support.

Reference

[1] R.C. Baetzold, J. Phys. Chem. B 101 (1997) 8180.
[2] S.A. Mitchell, G.A. Kenney-Wallace, G.A. Ozin, J. Am. Chem. Soc. 103 (1981) 6030.
[3] A. Vogler, H. Kunkely, Chem. Phys. Lett. 158 (1989) 74.
[4] G.W. Eastland, M.A. Mazid, D.R. Russell, M.C.R. Symons, J. Chem. Soc., Dalton Trans. (1980) 1682.
[5] Y. Kim, K. Seff, J. Am. Chem. Soc. 100 (1978) 6989.
[6] J. Michalik, T. Wasowicz, A. Van der Pol, E.J. Reijerse, E. De Boer, J. Chem. Soc., Chem. Commun. (1992) 29.
[7] G.A. Ozin, F. Hugues, J. Phys. Chem. 87 (1983) 94.
[8] M.A. Rawashdeh-Omary, M.A. Omary, H.H. Patterson, J. Am. Chem. Soc. 122 (2000) 10371.

[9] M.A. Rawashdeh-Omary, M.A. Omary, H.H. Patterson, J.P. Fackler Jr., J. Am. Chem. Soc. 123 (2001) 11237.
[10] T. Sun, K. Seff, Chem. Rev. 94 (1994) 857.
[11] M. Matsuoka, W.-S. Ju, H. Yamashita, M. Anpo, J. Photochem. Photobiol., A 160 (2003) 43.
[12] M. Matsuoka, W.S. Ju, H. Yamashita, M. Anpo, J. Synchrotron Radiat. 8 (2001) 613.
[13] M. Matsuoka, M. Anpo, NATO Science Series, II: Mathematics, Physics and Chemistry, vol. 13, 2001, p. 249.
[14] F. Zhang, N. Guan, Y. Li, X. Zhang, J. Chen, H. Zeng, Langmuir 19 (2003) 8230.
[15] M. Anpo, M. Matsuoka, H. Mishima, H. Yamashita, Res. Chem. Intermed. 23 (1997) 197.
[16] M. Anpo, Y. Shioya, H. Yamashita, E. Giamello, C. Morterra, M. Che, H.H. Patterson, S. Webber, S. Ouellette, et al. J. Phys. Chem. 98 (1994) 5744.
[17] M. Anpo, S.G. Zhang, M. Matsuoka, H. Yamashita, Catal. Today 39 (1997) 159.
[18] M. Anpo, M. Matsuoka, H. Yamashita, Catal. Today 35 (1997) 177.
[19] M. Anpo, S. Dohshi, M. Kitano, Y. Hu, Chem. Ind. 108 (2006) 595.
[20] M. Matsuoka, E. Matsuda, K. Tsuji, H. Yamashita, M. Anpo, J. Mol. Catal. A: Chem. 107 (1996) 399.
[21] W.S. Szulbinski, Inorg. Chim. Acta 269 (1998) 253.
[22] M.D. Baker, G.A. Ozin, J. Godber, J. Phys. Chem. 89 (1985) 305.
[23] F. Fang, S. Kanan, H.H. Patterson, C.S. Cronan, Anal. Chim. Acta 373 (1998) 139.
[24] J. Bachman, H.H. Patterson, Environ. Sci. Technol. 33 (1999) 874.
[25] A. Ghauch, C. Gallet, A. Charef, J. Rima, M. Martin-Bouyer, Chemosphere 42 (2001) 419.
[26] S.M. Kanan, C.P. Tripp, R.N. Austin, H.H. Patterson, J. Phys. Chem. B 105 (2001) 9441.
[27] M.C. Kanan, S.M. Kanan, H.H. Patterson, Res. Chem. Intermed. 29 (2003) 691.
[28] S.M. Kanan, M.C. Kanan, H.H. Patterson, Curr. Opin. Solid State Mater. Sci. 7 (2003) 443.
[29] M.C. Kanan, S.M. Kanan, R.N. Austin, H.H. Patterson, Environ. Sci. Technol. 37 (2003) 2280.
[30] V. Rakic, V. Rac, V. Dondur, A. Auroux, Catal. Today 110 (2005) 272.
[31] J.A.Z. Pieterse, G. Mul, I. Melian-Cabrera, R.W. Brink, Catal. Lett. 99 (2005) 41.
[32] M. Watanabe, H. Uchida, K. Ohkubo, H. Igarashi, J. Power Sources 46 (2003) 595.
[33] P.V. Samant, J.B. Fernandes, Appl. Catal. B 125 (2004) 172.
[34] M. Matsuoka, M. Anpo, J. Photochem. Photobiol. C 3 (2003) 225.
[35] A. Stem, G.A. Ozin, G. Stucky, J. Am. Chem. Soc. 114 (1992) 5171.
[36] A. Stem, G.A. Ozin, Advances in the Synthesis and Reactivity of Solids, vol. 2, JAI Press, Greenwich, CT, 1994, p. 93.
[37] T. Bein, F. Schmidt, W. Gunsser, G. Schmiester, Surf. Sci. 156 (1985) 57.
[38] M. Yee, I.I. Yaacob, J. Mater. Res. 19 (2004) 930.
[39] S.M. Kanan, M.C. Kanan, H.H. Patterson, J. Phys. Chem. B 105 (2001) 7508.
[40] G. Calzaferri, Proc. Int. Ninth Conf. Photochem. Photoelectrochem. Convers. Storage Sol. Energy, 1993, p. 141.
[41] H. Yamashita, M. Matsuoka, M. Anpo, M. Che, J. Phys. IV 7 (1997) 941.
[42] M. Anpo, Nuovo Cimento Soc. Ital. Fish. D 19D (1997) 1641.
[43] S.M. Kanan, M.A. Omary, H.H. Patterson, M. Matsuoka, M. Anpo, J. Phys. Chem. B 104 (2000) 3507.
[44] W.-S. Ju, M. Matsuoka, K. Iino, H. Yamashita, M. Anpo, J. Phys. Chem. B 108 (2004) 2128.
[45] S. Rodrigues, S. Uma, I.N. Martyanov, K.J. Klabunde, J. Catal. 233 (2005) 405.
[46] T. Kamegawa, R. Takeuchi, M. Matsuoka, M. Anpo, Catal. Today 111 (2006) 248.
[47] J.-S. Hwang, J.-S. Chang, S.-E. Park, K. Ikeue, M. Anpo, Top. Catal. 35 (2005) 311.
[48] M.A. Omary, H.H. Patterson, J. Am. Chem. Soc. 120 (1998) 7696.
[49] M.A. Omary, D.R. Hall, G.E. Shankle, A. Siemiarczuk, H.H. Patterson, J. Phys. Chem. B 103 (1999) 3845.
[50] M.A. Rawashdeh-Omary, M.A. Omary, G.E. Shankle, H.H. Patterson, J. Phys. Chem. B 104 (2000) 6143.
[51] M.A. Rawashdeh-Omary, C.L. Larochelle, H.H. Patterson, Inorg. Chem. 39 (2000) 4527.
[52] H.H. Patterson, S.M. Kanan, M.A. Omary, Coord. Chem. Rev. 208 (2000) 227.